Am J Transl Res 2026;18(5):4305-4313
www.ajtr.org /ISSN:1943-8141/AJTR0172871

Original Article

Application of ^{131}I-MIBG imaging in assessing renal sympathetic overdrive in heart failure with preserved ejection fraction (HFpEF)

Zhiqiang Yang[1], Yue Li[2], Pei Yin[3], Qingzhen Zhao[1], Yuzhi Zhen[1], Ruisi Liu[4], Lizhuo Li[1], Chao Liu[1]

[1]Heart Center, The First Hospital of Hebei Medical University, Shijiazhuang, Hebei, China; [2]Heart Center, The Second Hospital of Hebei Medical University, Shijiazhuang, Hebei, China; [3]Department of Nuclear Medicine, The First Hospital of Hebei Medical University, Shijiazhuang, Hebei, China; [4]Xiangya School of Public Health, Central South University, Changsha, Hunan, China

Received March 25, 2026; Accepted May 15, 2026; Epub May 15, 2026; Published May 30, 2026

Abstract: Objective: To quantitatively assess cardiac and renal sympathetic nerve activity using ^{131}I-metaiodobenzylguanidine (MIBG) imaging, in patients with heart failure with preserved ejection fraction (HFpEF) diagnosed via left heart catheterization, compared with matched controls. Methods: The study enrolled 18 HFpEF patients (diagnosed via left heart catheterization for exertional dyspnea as the test group) and 10 matched controls. All subjects underwent cardiac and renal ^{131}I-MIBG imaging. We measured early (15 min, reflecting nerve density/uptake) and delayed (4 h, reflecting neurotransmitter storage/turnover) kidney-to-mediastinum (K/M) and heart-to-mediastinum (H/M) ratios, as well as washout rates (WR). Results: Invasive hemodynamic measurements showed elevated mean left ventricular end-diastolic pressure (mLVEDP) in the test group [21 (18, 24) mmHg vs. 7.5 (5, 8) mmHg, $P < 0.05$]. Notably, ^{131}I-MIBG imaging indicated significantly higher renal sympathetic activation in the test group during both the early and delayed phases (K/M15min: 10.5 ± 2.5 vs. 3.7 ± 0.45 and K/M4h: 8.1 ± 3.3 vs. 4.6 ± 0.3, $P < 0.05$), the former being approximately two to three times greater than the latter. This hypersympathetic state significantly paralleled the elevation in LAD and mLVEDP ($P < 0.05$), indicating a direct link between renal neuro-overactivity and cardiac diastolic impairment. Conclusions: ^{131}I-MIBG imaging successfully quantifies renal-cardiac sympathetic crosstalk in HFpEF. The markedly elevated K/M ratios demonstrate that renal sympathetic overactivity is a core driver of hemodynamic congestion in these patients. Clinically, this technique may serve as a powerful non-invasive biomarker to identify candidates for sympatho-inhibitory therapies and provides a precise tool for monitoring therapeutic efficacy in HFpEF management.

Keywords: Heart failure with preserved ejection fraction, ^{131}I-MIBG imaging, sympathetic nervous activity

Introduction

Heart failure with preserved ejection fraction (HFpEF), also called diastolic heart failure, is a disease or syndrome with a strong tendency toward heterogeneity, and may result from the action of one or more disorders [1]. Chronic activation of the sympathetic nervous system elevates heart rate and myocardial contractility, thereby increasing myocardial energy demand. This can induce vascular stiffness, promote myocardial fibrosis, trigger arrhythmias, impair endothelial function, and ultimately accelerate the progression of myocardial dysfunction [2]. Yet, the majority of researches have concentrated on the cardiac sympathetic system, with relatively little attention given to activation of the renal sympathetic system, especially in HFpEF [3]. Given that the kidneys are the primary regulators of sodium balance and plasma volume, renal sympathetic overactivity directly triggers the renin-angiotensin-aldosterone system (RAAS) cascade, leading to fluid congestion and elevated filling pressures that define the HFpEF phenotype. Thus, quantifying renal-specific sympathetic drive is crucial for a comprehensive systemic understanding of the disease.

The ^{123}I-MIBG imaging technique utilizes the properties of metaiodobenzylguanidine (MIBG), a guanidine analogue that can be taken up by

https://doi.org/10.62347/OBPS4683

the synaptic vesicles of cardiac sympathetic nerve endings through the same mechanism as norepinephrine, enabling radiolabeling of norepinephrine receptor binding and thereby allowing non-invasive and quantitative assessment of the function and integrity of cardiac and renal sympathetic nerves [4]. In this context, the early-phase (15 min) imaging provides a measure of sympathetic nerve terminal density, while the delayed-phase (4 h) imaging reflects the functional dynamics of neurotransmitter storage and turnover, offering a comprehensive view of neuro-effector status. It is currently a reliable adjunct for clinical renal denervation in patients with hypertension [5]. Clinical trials have demonstrated the value of quantitative early- and delayed-phase parameters of cardiac ^{123}I-MIBG imaging in predicting adverse cardiac events long-term in patients with heart failure [6].

Despite characteristic changes in ^{123}I-MIBG uptake, distribution, and washout in the heart and kidney, its application in HFpEF has rarely been reported. In China, due to the limitations of ^{123}I-MIBG supply in China, we attempted to analyze sympathetic nerve activity and its distribution in the heart and kidney by replacing ^{123}I-MIBG with ^{131}I-MIBG [7]. Previous studies have demonstrated that ^{131}I-MIBG provides diagnostic accuracy comparable to that of ^{123}I-MIBG in quantifying sympathetic activity, making it a viable and reliable alternative in resource-limited clinical settings [8].

As is well known, the 15 min imaging mainly reflects the density of cardiac and renal sympathetic nerve endings; the 4 h imaging mainly reflects the functional activity of cardiac and renal sympathetic nerves; and the washout rate (WR) mainly reflects the storage function of vesicles in sympathetic nerve endings [9]. However, there is a lack of empirical data directly linking renal-specific sympathetic overactivity to invasive hemodynamic parameters in HFpEF patients. Filling this gap is essential for identifying physiological targets for emerging therapies like renal denervation (RDN).

Therefore, this study included patients with HFpEF who underwent left heart catheterization for diagnosis, as well as volunteers matched for age, sex, and blood pressure whose mean left ventricular end-diastolic pressure (mLVEDP) was < 10 mmHg. All participants underwent underwent ^{131}I-MIBG imaging to quantitatively assess cardiac and renal sympathetic nerve activity and to analyze its relationship with indicators of left ventricular structure and cardiac function obtained by echocardiography, in order to characterize cardiac and renal sympathetic nerve distribution and activity in patients with HFpEF. All enrolled subjects underwent cardiac and renal ^{131}I-MIBG imaging within one week after cardiac catheterization.

Methods

Patients

The study enrolled 18 consecutive patients diagnosed with diastolic heart failure (HFpEF) according to the ESC Guidelines for the Diagnosis and Management of Acute and Chronic Heart Failure 2021 [10]. These patients underwent left heart catheterization because of unexplained exertional dyspnea not attributable to respiratory diseases, formed the experimental group. The exclusion of respiratory conditions was confirmed in collaboration with the chief resident of respiratory medicine. Patients in the control group were matched for age, sex, and blood pressure. The experimental group comprised 9 females and 9 males, with a mean age of 56 years. Conversely, the control group included 6 females and 4 males, with an average age of 58 years.

Patients were excluded based on the following criteria: left ventricular ejection fraction (LVEF) less than 50% as indicated by echocardiography. Age < 18 years; coronary angiography revealing the need for intervention because of coronary stenosis; diagnosis of obstructive sleep apnea syndrome (OSAS), congenital heart disease, significant valvular heart disease (beyond mild stenosis or moderate regurgitation), pulmonary hypertension, constrictive pericarditis, primary cardiomyopathy, or prior heart transplantation, presence of severe infections, malignant tumors, or a life expectancy of less than one month; and severe hepatic or renal dysfunction [11].

All participants underwent comprehensive hemodynamic catheterization at Hebei Medical University to ensure that dyspnea was not related to pulmonary diseases.

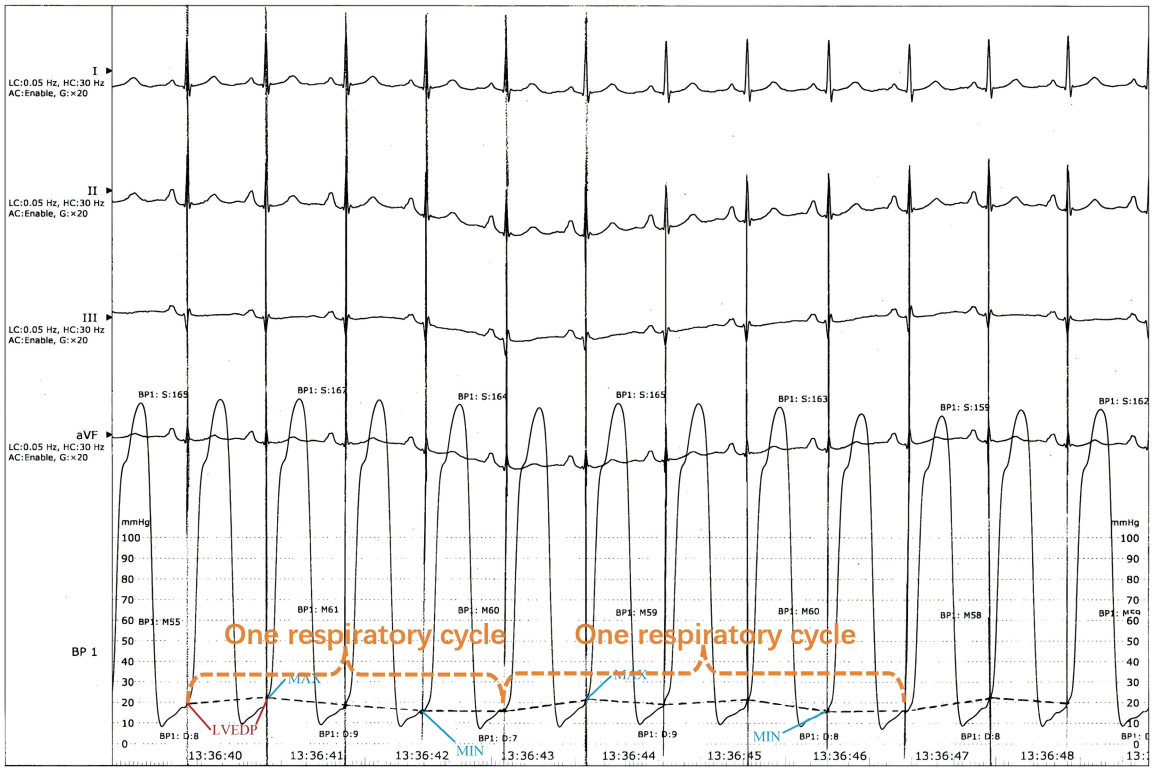

Figure 1. LVEDP measurement method using left cardiac catheterization. The image illustrates the methodology for determining LVEDP via left cardiac catheterization, displayed on a multichannel monitor. The key step involves identifying the peak of the R wave on the ECG component of the monitor, which marks the end of left ventricular diastole. A vertical line extending from the apex of the R wave intersects the left ventricular pressure waveform, pinpointing the instant at which LVEDP is measured. This intersection reveals the LVEDP, which is observed to fluctuate with respiratory cycles. The curve of LVEDP respiratory fluctuation shows a maximum and a minimum value during each respiratory cycle. The interval between two successive peaks, corresponding to maximum pressures, denotes a single respiratory cycle, demonstrates how LVEDP dynamically changes with respiration. LVEDP: left ventricular end-diastolic pressure.

Medical ethics

This study was approved by the Ethics Committee of the First Hospital of Hebei Medical University.

Experimental protocol

Subjects underwent ^{131}I-MIBG imaging within one week after cardiac catheterization. Cardiac ultrasound and other pertinent clinical data were collected during hospitalization.

Left heart catheterization

Under X-ray fluoroscopy, a 6F pigtail catheter was inserted into the left ventricle through the radial artery sheath, ensuring the catheter tip did not contact the left ventricular wall. A high-pressure pump facilitated left ventriculography to assess ventricular wall motion. Standardized calibration was performed to ensure the accuracy of invasive hemodynamic measurements. Left ventricular end-diastolic pressure (LVEDP) readings were adjusted using a level meter aligned with the mid-axillary line and the fourth intercostal space. Mean LVEDP (mLVEDP) was calculated as the average of five consecutive calm breathing cycles, avoiding breath-holding or Valsalva maneuvers. The mLVEDP and its variability ($mLVEDP_{max-min}$) were automatically recorded by a multicontact electrophysiologic recorder while accounting for the effects of respiratory rate and heart rate variability. The $mLVEDP_{max-min}$ represented the average difference between the maximum and minimum values across five consecutive resting respiratory cycles, as shown in **Figure 1**.

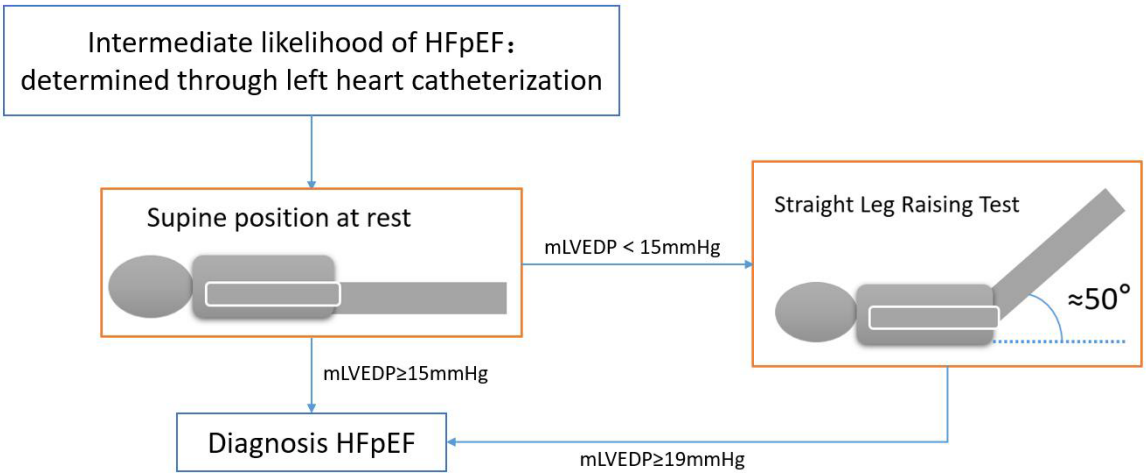

Figure 2. Clinical diagnosis of HFpEF. HFpEF: heart failure with preserved ejection fraction.

Diagnosing HFpEF with the straight leg raising test

The clinical diagnosis of HFpEF was refined by incorporating a straight leg raising test at approximately 50°, where an mLVEDP ≥ 19 mmHg indicated HFpEF if the resting mLVEDP < 15 mmHg. This method, illustrated in **Figure 2**, effectively identifies cryptogenic HFpEF with a specificity of 100%, independent of diuretic use [12].

Cardiac and renal ^{131}I-MIBG imaging

The procedures for cardiac and renal ^{131}I-MIBG imaging, as well as the reproducibility analysis of quantitative Heart and renal ^{131}I-MIBG imaging, are presented in the Supplementary Materials.

Statistical analysis

Data analysis was conducted using SPSS for Windows (version 22.0). Continuous variables with a normal distribution are presented as mean ± standard deviation, whereas non-normally distributed measures are described as median (P_{25}, P_{75}). Pearson correlation coefficients were used to examine relationships between normally distributed variables, whereas Spearman's rank correlation coefficients were used for non-normally distributed variables. Differences between groups for normally distributed data were analyzed using t-tests, whereas the Mann-Whitney U test was used for non-normally distributed data. Fisher's exact test was applied to compare categorical variables between groups. Bland-Altman analysis was used to evaluate intra- and inter-observer variability, as well as the reproducibility of ^{131}I-MIBG imaging results. Data visualization was supported by MedCalc and GraphPad Prism 2021. A *p*-value < 0.05 was considered statistically significant.

Results

As shown in **Table 1**, the control subjects were appropriately matched with the HFpEF group in terms of age, sex, and blood pressure, with no significant difference observed (age: 56 ± 10 vs. 58 ± 13, female: 50% vs. 60%, SBP: 130 ± 11 mmHg vs. 136 ± 10 mmHg, DBP: 84 ± 6.8 mmHg vs. 81 ± 11 mmHg, $P > 0.05$). The HFpEF group exhibited a higher E/e' ratio than the control group (11 ± 2 vs. 5 ± 0.9, $P < 0.05$), indicating more severe diastolic dysfunction. Invasive hemodynamic measurements revealed that both mLVEDP and its variability $mLVEDP_{max-min}$, were significantly higher in the HFpEF group [21 (18, 24) mmHg vs. 7.5 (5, 8) mmHg, 10 (7, 12) mmHg vs. 5 (3, 7) mmHg, respectively; $P < 0.05$], serving as the primary criteria for participant grouping. All participants had hypertension, with HFpEF patients requiring a broader range of medications for blood pressure management (3 vs. 2, $P < 0.05$).

Analysis of ^{131}I-MIBG imaging, as detailed in **Tables 2** and **3**, indicated no significant differences in the early and delayed heart-to-medias-

Table 1. Baseline characteristics

	HFpEF (N=18)	Non-HFpEF (N=10)	χ^2/t	*P*
Age (years)	57.3 ± 13.2	54.7 ± 13.8	0.489	0.629
Female (%)	9 (50)	6 (60)	0.289	0.611
Weight (kg)	74.8 ± 17.4	65.8 ± 11.3	1.461	0.156
BMI (kg/m^2)	28.1 ± 4.7	24.9 ± 3.9	1.862	0.074
BNP (ng/L)	30.0 (16.5, 108.5)	11.0 (8.4, 18.5)	0.891	< 0.0001
eGFR (ml/min/1.73 m^2)	89.5 (81.6, 105.1)	90.9 (83.8, 97.6)	0.691	0.495
SBP (mmHg)	132.7 ± 10.1	134.9 ± 9.5	0.559	0.581
DBP (mmHg)	84.0 ± 7.1	81.3 ± 10.8	0.802	0.430
NYHA class (%)			-	-
I	0 (0)	0 (0)		
II	7 (50)	0 (0)		
III	4 (29)	0 (0)		
IV	3 (21)	0 (0)		
mLVEDP (mmHg)	19.5 (18.0, 21.8)	6.5 (5.0, 8.0)	8.594	< 0.0001
$mLVEDP_{max-min}$	10.0 (9.3, 10.0)	5.0 (5.0, 6.0)	9.143	< 0.0001
Complications				
Hypertension (%)	18 (100)	10 (100)		-
Atrial fibrillation (%)	5 (27)	0 (0)	3.382	0.066
Type 2 diabetes (%)	8 (44)	1 (10)	3.497	0.062
Cardiac ultrasound				
LVEF (%)	62 ± 5.4	63 ± 2.6	0.548	0.588
LAD (mm)	37 ± 6.5	30 ± 2.8	3.222	0.003
E/e'	11 ± 2	5 ± 0.9	8.940	0.000
Medication (%)				
ACEI/ARB	7 (38)	5 (50)	0.324	0.569
β blocker	15 (83)	3 (30)	7.964	0.005
Calcium antagonist (%)	6 (33)	3 (30)	0.033	0.856
Diuretic	10 (55)	0 (0)	8.642	0.003
Number of antihypertensive drug types	3 (3, 5)	2 (2, 2)	3.691	0.001
New coronavirus infection (%)	9 (50)	6 (60)	0.289	0.611

Notes: BMI: body mass index; BNP: brain natriuretic peptide; eGFR: estimate the glomerular filtration rate; SBP: systolic blood pressure; DBP: diastolic blood pressure; NYHA: New York heart association; mLVEDP: mean left ventricular end-diastolic pressure; LVEF: left ventricular ejection fraction; LAD: anterior-posterior left atrial diameters; ACEI/AEB: angiotensin-converting enzyme inhibitor/angiotensin II receptor antagonist.

Table 2. Results of cardiac ^{131}I-MIBG imaging

Heart ^{131}I-MIBG	HFpEF (N=18)	Non-HFpEF (N=10)	t	*P*
15 min H/M	2.1 ± 0.3	2.0 ± 0.2	0.940	0.356
4 h H/M	2.0 ± 0.2	1.9 ± 0.2	1.268	0.216
WR (%)	36 ± 3.3	28 ± 1.8	7.065	0.000

Notes: HFpEF: heart failure with preserved ejection fraction; MIBG: metaiodobenzylguanidine; H/M: heart-to-mediastinum; WR: washout rates.

tinum (H/M) ratios (H/M15min: 2.1 ± 0.3 vs. 2.0 ± 0.2, and H/M4h: 2.0 ± 0.2 vs. 1.9 ± 0.2, $P > 0.05$). However, the kidney-to-mediastinum (K/M) ratios in both the early and delayed phases were significantly higher in the HFpEF group, approximately two- to three-fold greater than those in the control group (K/M15min: 10.5 ± 2.5 vs. 3.7 ± 0.45, and K/M4h: 8.1 ± 3.3 vs. 4.6 ± 0.3, $P < 0.05$). The renal washout rate (WR) was lower in the HFpEF group (52 ± 2.1% vs. 56 ± 3.2%, P=0.000).

Semi-quantitative ROI analysis of bilateral renal radioactivity counts

As shown in **Figure 3**, rainbow-mode analysis revealed that the HFpEF group exhibited higher renal radioactivity than the non-HFpEF group during both the early and delayed phases,

Table 3. Results of kidney ^{131}I-MIBG imaging

Kidney ^{131}I-MIBG	HFpEF (N=18)	Non-HFpEF (N=10)	t	*P*
Left kidney 15 min K/M	10 ± 3.0	3.6 ± 0.5	6.641	0.000
Right kidney 15 min K/M	11.7 ± 2.0	3.9 ± 0.4	12.10	0.000
Left kidney 4 h K/M	8.3 ± 3.1	4.8 ± 0.4	3.525	0.002
Right kidney 4 h K/M	8 ± 3.5	4.5 ± 0.2	3.133	0.004
WR (%)	52 ± 2.1	56 ± 3.2	4.000	0.000

Notes: HFpEF: heart failure with preserved ejection fraction; MIBG: metaiodobenzylguanidine; K/M: kidney-to-mediastinum; WR: washout rates.

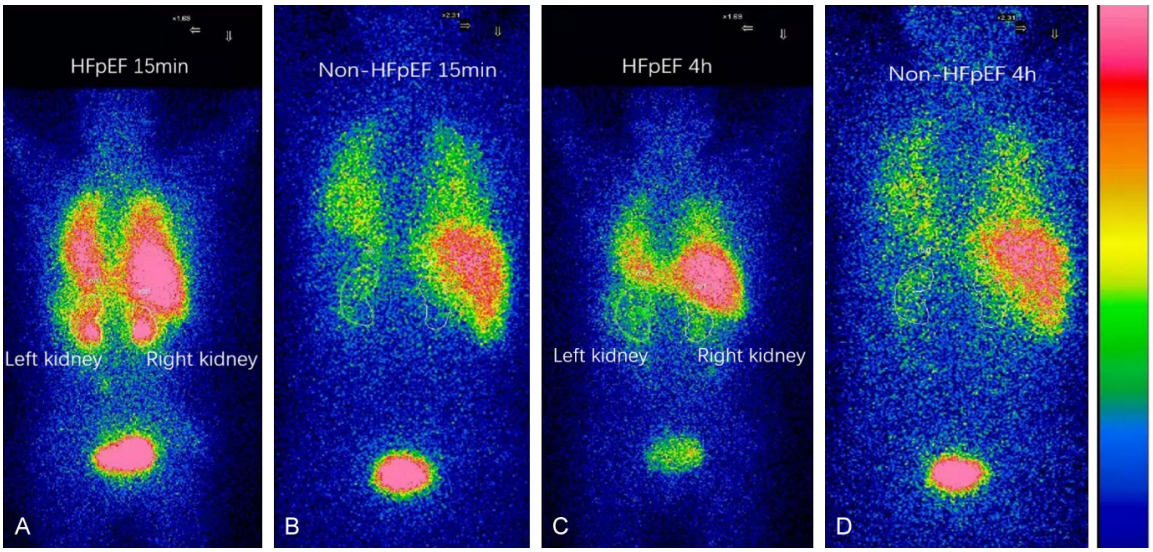

Figure 3. Semi-quantitative analysis of 15-min and 4-h radioactivity counts of both kidneys in rainbow mode. A and B. Depict the ROIs for the early phases of kidney imaging in patients with HFpEF and non-HFpEF. C and D. Illustrate the ROIs for the kidneys during the delayed phases of kidney imaging, respectively. The scale on the right represents ^{131}I-MIBG imaging in rainbow mode corrected using the same contrast standard. HFpEF: heart failure with preserved ejection fraction.

underscoring enhanced sympathetic activity in the kidneys of HFpEF patients.

Quantitative ROI analysis of bilateral renal radioactivity counts

As shown in **Tables 2** and **3** and **Figure 4**, further analysis comparing the mean bilateral renal R/H ratios at 15 min and 4 h post-injection revealed that the HFpEF group had significantly higher R/H ratios than the non-HFpEF group in both the early and delayed phases. The former was approximately two to three times greater than the latter (K/M15min: 10.5 ± 2.5 vs. 3.7 ± 0.45, and K/M4h: 8.1 ± 3.3 vs. 4.6 ± 0.3, $P < 0.05$). These findings indicate heightened renal sympathetic activity in patients with HFpEF.

Comparison of mLVEDP and mLVEDP variability

Analysis revealed a significant difference in mLVEDP between the HFpEF and the control groups [21 (18, 24) mmHg vs. 7.5 (5, 8) mmHg, $P < 0.01$] (**Figure 5A**). Additionally, the variability of mLVEDP, measured as the difference between maximum and minimum values ($mLVEDP_{max-min}$), also showed a statistically significant difference between the two groups [10 (7, 12) mmHg vs. 5 (3, 7) mmHg, $P < 0.05$] (**Figure 5B**). The significant difference in $mLVEDP_{max-min}$ between HFpEF and control groups further suggests underlying depletion of cardiac functional reserve in HFpEF patients, warranting further investigation under hemodynamic stress conditions [12].

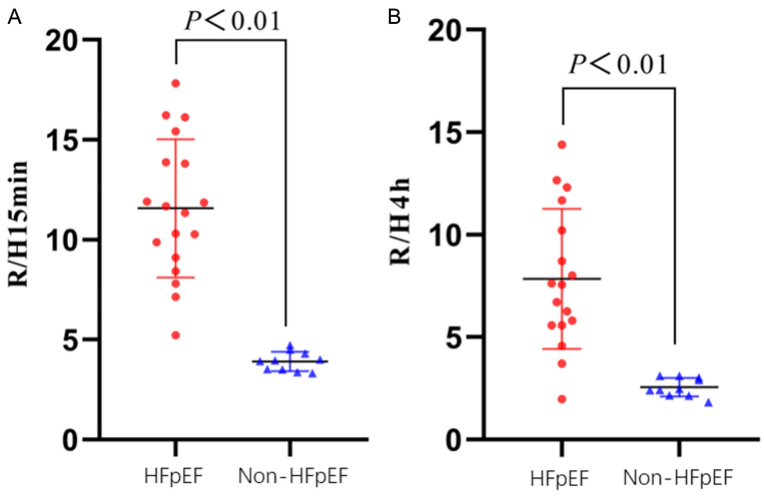

Figure 4. Comparison of mean values of bilateral renal R/H values. A. R/H ratio in 15 min between two groups; B. R/H ratio in 4 hours between two groups. R/H: renal to heart; HFpEF: heart failure with preserved ejection fraction.

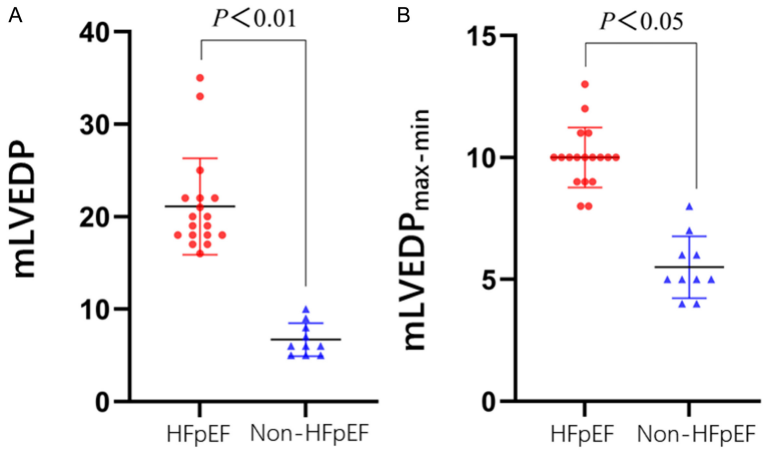

Figure 5. Comparison of mLVEDP and mLVEDP variability. A. mLVEDP beween two groups; B. mLVEDP variability beween two groups. The $mLVEDP_{max-min}$, which indicates the variability of mLVEDP, represents the average difference between the maximum and minimum values across five consecutive resting respiratory cycles Comparison of mLVEDP and mLVEDP Variability. mLVEDP: mean left ventricular end-diastolic pressure.

Discussion

The interplay between cardiovascular neuromodulation and heart failure progression underscores the critical role of sympathetic overactivation in patient outcomes, as initially proposed by Prof. Floras in 2009 [13]. Although initially adaptive, this sympathetic response eventually becomes deleterious and is compounded by diminished vagal reflexes that fail to buffer sympathetic outflow [14]. Renal denervation studies in rats and clinical trials have echoed these findings, highlighting the link between excessive sympathetic activity and the development of heart failure [15, 16].

Quantitative analysis of renal sympathetic nerve activity using ^{131}I-MIBG imaging underscores the heightened sympathetic activation in HFpEF patients compared with controls, affirming the role of renal sympathetic system overactivation in HFpEF [17].

HFpEF, constituting approximately half of all heart failure cases, has emerged as a major research focus over the past decade [18]. Despite initial perceptions of HFpEF as a less severe form of heart failure, recent studies suggest that it has become the predominant type of heart failure, challenging previous expectations regarding morbidity and mortality [19]. HFpEF is characterized by impaired myocardial relaxation and compliance, leading to congestive heart failure because of ineffective diastolic filling and increased left-sided cardiac loading [20]. Hypertension, a leading cause of HFpEF, exacerbates left ventricular diastolic dysfunction and increases cardiac mass due to chronic intraventricular pressure overload [21]. Abnormal sympathetic nervous system (SNS) activation is pivotal in the development and prognosis of HFpEF's , with both preclinical and clinical studies underscoring the role of SNS hyperactivation irrespective of hypertension [22, 23].

Novelty of our findings

Our study is the first to delineate the critical role of SNS overactivity in HFpEF, representing a significant advancement in understanding

the pathophysiological mechanisms underlying this condition. As shown in **Tables 2** and **3** and **Figure 3**, by semi-quantitatively and quantitatively assessing cardiac and renal sympathetic nerve activity through ^{131}I-MIBG imaging in HFpEF patients, we unveiled a previously underrecognized aspect of HFpEF that may have substantial implications for its management and treatment strategies.

Implications for renal sympathetic denervation

Moreover, our findings highlight the potential of renal sympathetic denervation as a promising therapeutic strategy for patients with HFpEF. The significantly increased renal sympathetic activity observed in HFpEF patients compared with controls not only underscores the impact of SNS hyperactivation on the development of HFpEF but also suggests that targeting this overactivity through renal denervation may offer a novel avenue for alleviating HFpEF symptoms and improving patient outcomes.

Correlation analysis is presented in the Supplementary Materials.

Limitations

Limited by the availability of ^{123}I-MIBG in China, we attempted to analyze sympathetic nerve activity and its distribution in the heart and kidney using ^{131}I-MIBG imaging. In addition, the findings of this single-center retrospective case-control study are constrained by its limited sample size and the high cost and limited accessibility of ^{131}I-MIBG imaging. The consistent use of antihypertensive medications among participants and the reluctance to discontinue these medications may also have influenced the study outcomes.

Conclusion

Quantitative analysis of renal sympathetic nerve activity using ^{131}I-MIBG imaging suggests that sympathetic activation in HFpEF patients is markedly increased compared with that in normal controls, with the former being approximately two to three times greater than the latter. These findings further suggest that patients with HFpEF may benefit from renal denervation.

Acknowledgements

We gratefully acknowledge the guidance of KunShen Liu, MD, PhD and Pei Yin, MD from the First Hospital of Hebei Medical University. This work was accomplished with the support of the Nature Fund of Hebei Province (No. H2021206180) in China.

Disclosure of conflict of interest

None.

Address correspondence to: Dr. Chao Liu, The First Hospital of Hebei Medical University, Hebei Medical University, 89 Donggang Road, Shijiazhuang 050031, Hebei, China. Tel: +86-031-187155262; Fax: +86-18633889667; ORCID: 0000-0002-5323-6733; E-mail: Liuchao@hebmu.edu.cn

References

[1] Ge J. Coding proposal on phenotyping heart failure with preserved ejection fraction: a practical tool for facilitating etiology-oriented therapy. Cardiol J 2020; 27: 97-98.

[2] Aikawa T, Naya M, Obara M, Manabe O, Tomiyama Y, Magota K, Yamada S, Katoh C, Tamaki N and Tsutsui H. Impaired myocardial sympathetic innervation is associated with diastolic dysfunction in heart failure with preserved ejection fraction: (11)C-Hydroxyephedrine PET study. J Nucl Med 2017; 58: 784-790.

[3] Merlet P, Pouillart F, Dubois-Randé JL, Delahaye N, Fumey R, Castaigne A and Syrota A. Sympathetic nerve alterations assessed with 123I-MIBG in the failing human heart. J Nucl Med 1999; 40: 224-231.

[4] Chen J, Folks RD, Verdes L, Manatunga DN, Jacobson AF and Garcia EV. Quantitative I-123 mIBG SPECT in differentiating abnormal and normal mIBG myocardial uptake. J Nucl Cardiol 2012; 19: 92-99.

[5] Dobrowolski LC, Eeftinck Schattenkerk DW, Krediet CTP, Van Brussel PM, Vogt L, Bemelman FJ, Reekers JA, Van Den Born BH and Verberne HJ. Renal sympathetic nerve activity after catheter-based renal denervation. EJNMMI Res 2018; 8: 8.

[6] Liga R, Gimelli A, Marzullo P, Ambrosio G, Cameli M, Cerbai E, Coiro S, Emdin M, Marcucci R, Morrone D, Palazzuoli A, Petronio AS, Savino K, Padeletti L and Pedrinelli R; Società Italiana di Cardiologia, Sezione Regionale Tosco-Umbra. Myocardial (123)I-metaiodobenzylguanidine imaging in hypertension and left ventricu-

lar hypertrophy. J Nucl Cardiol 2018; 25: 461-470.
[7] Ali N, Sebastian C, Foley RR, Murray I, Canizales AL, Jenkins PJ, Drake WM, Plowman PN, Besser GM, Chew SL, Grossman AB, Monson JP and Britton KE. The management of differentiated thyroid cancer using 123I for imaging to assess the need for 131I therapy. Nucl Med Commun 2006; 27: 165-169.
[8] Yang T, Wang L, Li Y, Cheng M, Jiao J, Wang Q and Guo H. (131)I-MIBG myocardial scintigraphy for differentiation of Parkinson's disease from multiple system atrophy or essential tremor in Chinese population. J Neurol Sci 2017; 373: 48-51.
[9] Noh MR, Jang HS, Kim J and Padanilam BJ. Renal sympathetic nerve-derived signaling in acute and chronic kidney diseases. Int J Mol Sci 2020; 21: 1647.
[10] McDonagh TA, Metra M, Adamo M, Gardner RS, Baumbach A, Böhm M, Burri H, Butler J, Čelutkienė J, Chioncel O, Cleland JGF, Coats AJS, Crespo-Leiro MG, Farmakis D, Gilard M, Heymans S, Hoes AW, Jaarsma T, Jankowska EA, Lainscak M, Lam CSP, Lyon AR, McMurray JJV, Mebazaa A, Mindham R, Muneretto C, Francesco Piepoli M, Price S, Rosano GMC, Ruschitzka F and Kathrine Skibelund A; ESC Scientific Document Group. 2021 ESC Guidelines for the diagnosis and treatment of acute and chronic heart failure. Eur Heart J 2021; 42: 3599-3726.
[11] Patel KP, Katsurada K and Zheng H. Cardiorenal syndrome: the role of neural connections between the heart and the kidneys. Circ Res 2022; 130: 1601-1617.
[12] Baratto C, Minari S, Rao VN, Soranna D, Zambon A, Perego GB, Paleari S, Senni M, Parati G, Vachiéry JL, Carnicelli AP, Houston BA, Taylor EA, Biscopink A, Tedford RJ and Caravita S. Diagnostic performance of passive leg-raise and low-workload exercise to diagnose heart failure with preserved ejection fraction. J Card Fail 2025; 31: 1675-1683.
[13] Floras JS. Sympathetic nervous system activation in human heart failure: clinical implications of an updated model. J Am Coll Cardiol 2009; 54: 375-385.
[14] Grassi G, Seravalle G, Quarti-Trevano F, Dell'Oro R, Arenare F, Spaziani D and Mancia G. Sympathetic and baroreflex cardiovascular control in hypertension-related left ventricular dysfunction. Hypertension 2009; 53: 205-209.
[15] Zheng H, Liu X, Katsurada K and Patel KP. Renal denervation improves sodium excretion in rats with chronic heart failure: effects on expression of renal ENaC and AQP2. Am J Physiol Heart Circ Physiol 2019; 317: H958-H968.
[16] Seravalle G, D'Arrigo G, Tripepi G, Mallamaci F, Brambilla G, Mancia G, Grassi G and Zoccali C. Sympathetic nerve traffic and blood pressure changes after bilateral renal denervation in resistant hypertension: a time-integrated analysis. Nephrol Dial Transplant 2017; 32: 1351-1356.
[17] Agostini D, Ananthasubramaniam K, Chandna H, Friberg L, Hudnut A, Koren M, Miyamoto MI, Senior R, Shah M, Travin MI, Dahl JV, Chen K and Levy WC; ADMIRE-HF investigators. Prognostic usefulness of planar (123)I-MIBG scintigraphic images of myocardial sympathetic innervation in congestive heart failure: follow-up data from ADMIRE-HF. J Nucl Cardiol 2021; 28: 1490-1503.
[18] Desai AS, Lam CSP, McMurray JJV and Redfield MM. How to manage heart failure with preserved ejection fraction: practical guidance for clinicians. JACC Heart Fail 2023; 11: 619-636.
[19] Wu X, Zhang T, Qiao J, Li C, Lin C and Xiong S. Effects of Kangdaxin on myocardial fibrosis in heart failure with preserved ejection fraction rats. J Thorac Dis 2022; 14: 1157-1163.
[20] Verbrugge FH, Omote K, Reddy YNV, Sorimachi H, Obokata M and Borlaug BA. Heart failure with preserved ejection fraction in patients with normal natriuretic peptide levels is associated with increased morbidity and mortality. Eur Heart J 2022; 43: 1941-1951.
[21] Zile MR, Baicu CF and Gaasch WH. Diastolic heart failure--abnormalities in active relaxation and passive stiffness of the left ventricle. N Engl J Med 2004; 350: 1953-1959.
[22] Ter Maaten JM, Damman K, Verhaar MC, Paulus WJ, Duncker DJ, Cheng C, van Heerebeek L, Hillege HL, Lam CS, Navis G and Voors AA. Connecting heart failure with preserved ejection fraction and renal dysfunction: the role of endothelial dysfunction and inflammation. Eur J Heart Fail 2016; 18: 588-598.
[23] Pandey A, Kraus WE, Brubaker PH and Kitzman DW. Healthy aging and cardiovascular function: invasive hemodynamics during rest and exercise in 104 healthy volunteers. JACC Heart Fail 2020; 8: 111-121.

Supplementary Materials

Cardiac and renal ^{131}I-MIBG imaging

To protect the thyroid gland from ^{131}I uptake, participants received 0.30-0.50 ml of compound iodine solution three times daily, starting three days prior to the imaging procedure and continuing for one week afterwards. Those on anti-hypertension medications maintained their regimen throughout the study. For imaging, subjects were administered 3 mCi of ^{131}I-MIBG through a bolus injection into the elbow vein. Anterior planar whole-body images were captured using a Precedence 6 SPECT/CT imaging system (PHILIPS, Netherlands) at 15 minutes and 4 hours post-injection.

As shown in Supplementary Figure 1, the heart-to-mediastinum (H/M) and kidney-to-mediastinum (K/M) radioactivity count ratios were determined by identifying the regions of interest (ROI) that highlighted the myocardial and renal uptake rates of ^{131}I-MIBG. The washout rates (WR) for both the heart and kidneys was calculated based on the early and delayed phase radioactivity counts. To ensure accuracy, ROI delineation for cardiac and renal imaging was independently performed twice by two experienced radiologists.

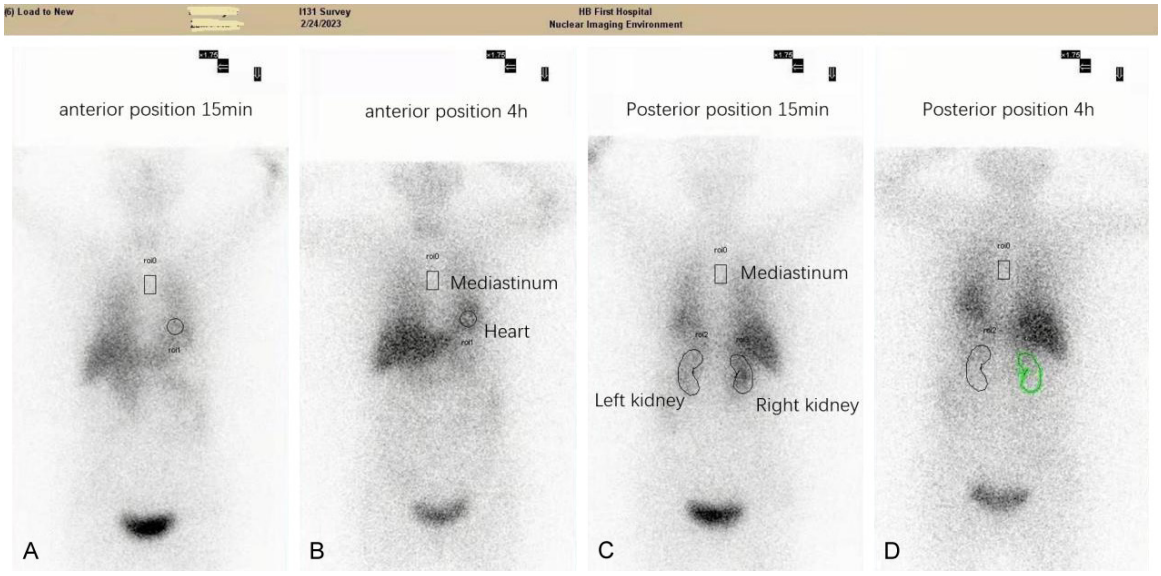

Supplementary Figure 1. ROIs of heart and kidney. (A and B) depict the anterior position SPECT camera acquisitions for the heart, highlighting the regions of interest (ROIs) drawn for the 15-minute and 4-hour post-injection time points, respectively. (C and D) showcase the posterior position SPECT camera acquisitions for the kidneys, with ROIs similarly drawn for the 15-minute and 4-hour intervals.

Reproducibility of quantitative heart and renal ^{131}I-MIBG imaging

Bland-Altman analysis showed acceptable reproducibility of calculating ^{131}I-MIBG heart and renal washout. As shown in Supplementary Figure 2, the limits of agreement for inter-and intra-observer reproducibility of repeat processing of WR of heart from 28 images were 9.0% (r=0.92) and 8.9% (r=0.93), and of kidney were 8.7% (r=0.95) and 8.8% (r=0.94), respectively.

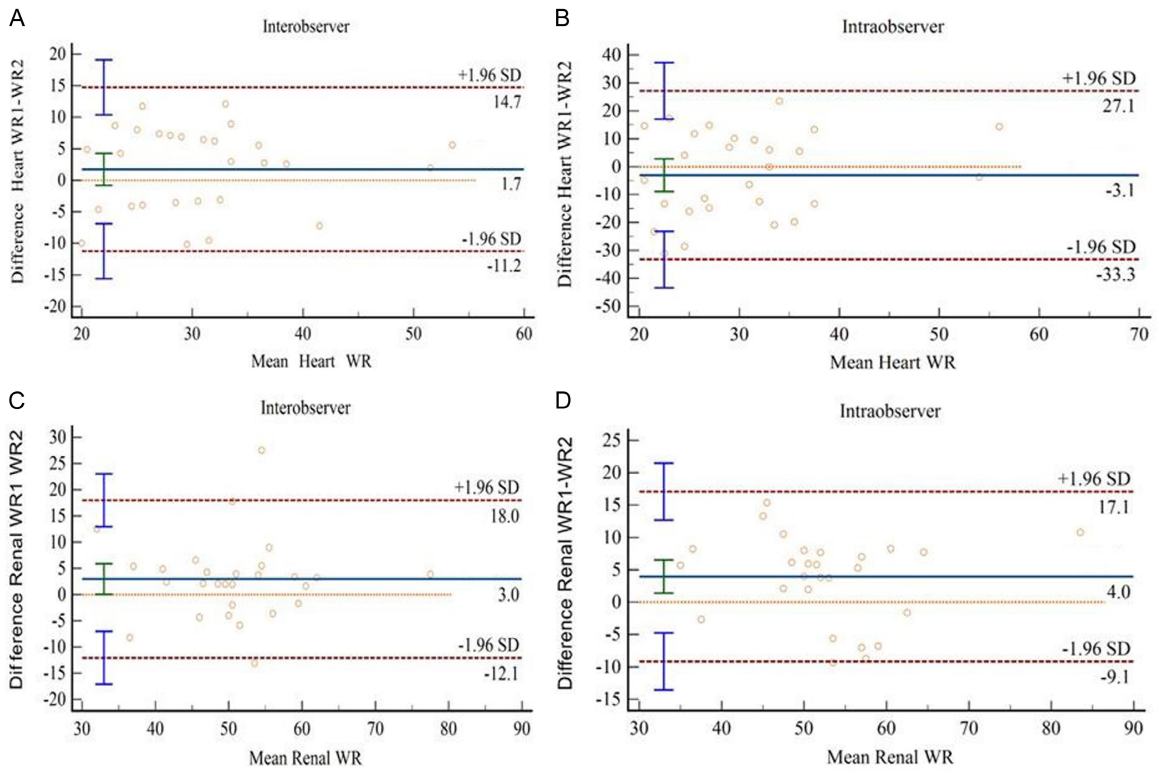

Supplementary Figure 2. Bland-Altman analyses. (A and B) present the Bland-Altman analyses for intra-observer variability, while (C and D) illustrate the inter-observer variability of ^{131}I-MIBG WR in the heart and kidneys among the 28 patients, respectively. The analyses' central point marks the mean difference between the two WR assessments. The upper and lower red dashed lines define the limits of agreement, set at 1.96 standard deviations (SD) from the mean.

Correlation analysis

As shown in Supplementary Figure 3, by Pearson analysis of the baseline data of all enrolled patients we found that E/e' and the anteroposterior diameter of the left atrium (LAD) showed a positive correlation (r=0.65). As shown in Supplementary Figure 4, through the study we also found that LVEDP in HFpFF patients showed a positive correlation with E/e' (ρ=0.50). Cardiorenal sympathetic activation was synchronized in both early and delayed phases (a positive correlation, ρ=0.52), which shows that systemic sympathetic overdrive in HFpEF patients, potentially moderated by the use of selective β_1 blockers. Additionally, renal WR correlate positively (ρ=0.56)with early-phase K/M ratios, indicating increased norepinephrine reuptake by renal sympathetic nerve endings, a key factor in the observed radioactivity increase in HFpEF patients' kidneys [1].

Interestingly, brain natriuretic peptide (BNP) levels in HFpEF patients do not align with the severity of congestive symptoms, suggesting a possible BNP deficiency or insensitivity in this population. The evolving understanding of HFpEF's inflammatory underpinnings, distinct from heart failure with reduced ejection fraction, calls for reevaluation of diagnostic and therapeutic strategies, including the role of BNP and the efficacy of renal denervation [2].

As shown in Supplementary Figure 4, our findings on the correlation between LVEDP and E/e' ratios, alongside the observed increase in left atrial anteroposterior diameter, underscore the complex pathophysiology of HFpEF and the potential for symptomatic progression due to compromised cardiac functional reserve [3].

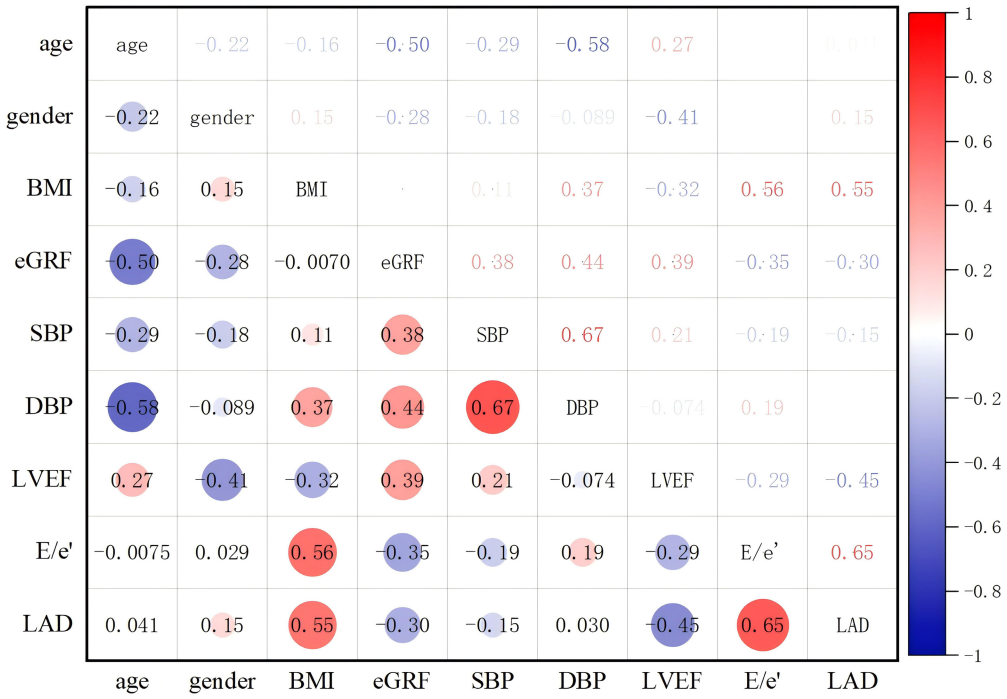

Supplementary Figure 3. Pearson correlation analysis of baseline data. LAD: anteroposterior diameter of the left atrium. The Pearson correlation coefficient is denoted by r.

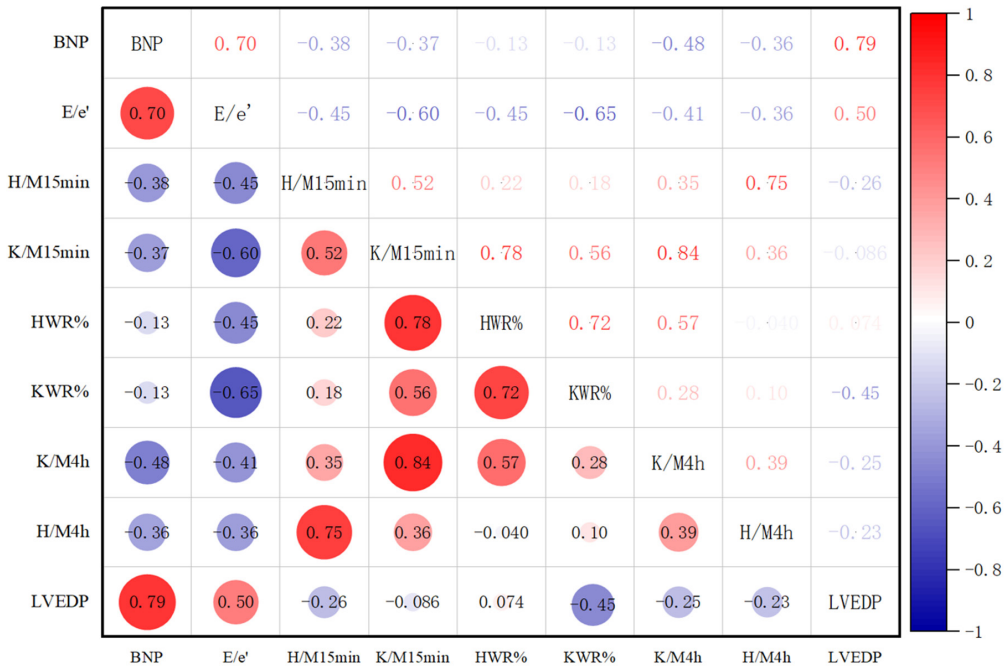

Supplementary Figure 4. Spearman correlation analysis of the HFpEF group. HWR%: washout rate of heart; KWR%: washout rate of kidney. The Spearman correlation coefficient is denoted by ρ. The red circle in Supplementary Figures 3 and 4 represents positive correlation, the blue circle represents negative correlation, and the darker the color, the stronger the correlation, and vice versa. The number on the top right of the image represents the corresponding correlation coefficient.

References

[1] van Veldhuisen DJ, Cohen-Solal A, Böhm M, Anker SD, Babalis D, Roughton M, Coats AJ, Poole-Wilson PA and Flather MD; SENIORS Investigators. Beta-blockade with nebivolol in elderly heart failure patients with impaired and preserved left ventricular ejection fraction: data from SENIORS (Study of Effects of Nebivolol Intervention on Outcomes and Rehospitalization in Seniors With Heart Failure). J Am Coll Cardiol 2009; 53: 2150-2158.

[2] Goetze JP, Bruneau BG, Ramos HR, Ogawa T, de Bold MK and de Bold AJ. Cardiac natriuretic peptides. Nat Rev Cardiol 2020; 17: 698-717.

[3] Bachmann KN, Gupta DK, Xu M, Brittain E, Farber-Eger E, Arora P, Collins S, Wells QS and Wang TJ. Unexpectedly low natriuretic peptide levels in patients with heart failure. JACC Heart Fail 2021; 9: 192-200.